Comparison of protective effects of trimetazidine against experimental warm ischemia of different durations: early and long-term effects in a pig kidney model

Christophe Jayle,[1] Frederic Favreau,[1] Kequiang Zhang,[1] Carole Doucet,[1] Jean Michel Goujon,[1] William Hebrard,[2] Michel Carretier,[1] Michel Eugene,[1] Gerard Mauco,[1] Jean Paul Tillement,[3] and Thierry Hauet[1,2]

[1]*Institut National de la Santé et de la Recherche Médicale E0324, Centre Hospitalier et Universitaire de Poitiers, Poitiers;* [2]*INRA, Unité de Transplantation Expérimentale, Département de Génétique Animale, Surgères; and* [3]*Laboratoire de Pharmacologie, Faculté de Médecine, Université Paris XII, Créteil, France*

Jayle C, Favreau F, Zhang K, Doucet C, Goujon JM, Hebrard W, Carretier M, Eugene M, Mauco G, Tillement JP, Hauet T. Comparison of protective effects of trimetazidine against experimental warm ischemia of different durations: early and long-term effects in a pig kidney model. *Am J Physiol Renal Physiol* 292: F1082–F1093, 2007; doi:10.1152/ajprenal.00338.2006.—Acute renal failure (ARF) is often the consequence of an ischemia-reperfusion injury (IRI) and associated with high mortality. Warm ischemia (WI) is a crucial factor of tissue damage, and tissue destruction led by ischemia-reperfusion (I/R) can impact the early and long-term functional outcome. Trimetazidine (TMZ) is an anti-ischemic drug. Previously, we already verified its protective effect on a cold-ischemic pig kidney model by directly adding TMZ into the preservation solution (Faure JP, Baumert H, Han Z, Goujon JM, Favreau F, Dutheil D, Petit I, Barriere M, Tallineau C, Tillement JP, Carretier M, Mauco G, Papadopoulos V, Hauet T. *Biochem Pharmacol* 66: 2241–2250, 2003; Faure JP, Petit I, Zhang K, Dutheil D, Doucet C, Favreau F, Eugene M, Goujon JM, Tillement JP, Mauco G, Vandewalle A, Hauet T. *Am J Transplant* 4: 495–504, 2004). In this study, we aimed to study the potential effect of TMZ pretreatment (5 mg/kg iv 24 h before WI) on the injury caused by WI for 45, 60, and 90 min and reperfusion in a WI pig kidney model. Compared with sham-operated (control) and uninephrectomized animals (UNX), TMZ pretreatment significantly reduced deleterious effects after 45 min, and particularly 60 and 90 min, of WI by improving the recovery of renal function and minimizing the inflammatory response commonly prevalent in ischemic kidney injury. Compared with controls (control group and UNX group), it was observed that *1*) hypoxia-inducible factor-1 (HIF-1α) expression occurred earlier and with a higher intensity in the TMZ-treated groups; *2*) the reduction of IRI during the first week following reperfusion was correlated with an earlier and greater expression of stathmin, which is involved in the process of tubular repair; and *3*) the tubulointerstitial fibrosis was reduced, particularly after 60 and 90 min of WI. In conclusion, TMZ made the warm-ischemic kidneys more resistant to the deleterious impact of a single episode of I/R and reduced early and long-term subsequent damage.

mitochondrial damage; ischemia-reperfusion injury; stathmin; renal regeneration

ACUTE RENAL FAILURE (ARF) is a clinical syndrome defined as an acute loss of renal function and is associated with high morbidity and mortality (27, 34). Postischemic renal failure is a severe outcome mostly observed after cadaveric renal transplantation, hemorrhagic shock, or sepsis. Ischemia-reperfusion injury (IRI) is a multifactorial process that has both immediate and long-term effects. Mitochondria take a critical part in it due to their role in tubule cell metabolism, generation of reactive oxygen species (ROS), and the initiation of apoptosis. Consequently, agents which could act on this organite are interesting therapeutic tools (18, 22). Moreover, the vascular endothelium is also a key site of injury from ROS and endothelial cell dysfunction is central to the pathogenesis of chronic allograft nephropathy (2, 3). We have previously evidenced the protective effect of TMZ on kidney grafts from cold preservation and reperfusion, showing that TMZ was efficient when added to various currently used preservation solutions (11, 12). Several reports have described different pharmacological effects of TMZ which are relevant in the prevention of organ damage from IRI: partial inhibition of fatty acid β-oxidation (20), reduction of ionic imbalance during ischemia-reperfusion (I/R) (9), increase in phospholipid uptake turnover (33), and membrane protection against reoxygenation-induced stress (32, 28). Other studies have showed that TMZ reduces intracellular acidosis, preserves ATP synthesis, limits inflammatory processes, and therefore ROS generation, and prevents Ca^{2+} overload (for a review, see Ref. 23). A recent study has identified the TMZ protective effect against different oxidizing systems, namely, Cu, Fe/ascorbate, and met-myoglobin/H_2O_2 (34). It was suggested that TMZ could act as a metal chelator of the permeability transition (34) and that TMZ inhibits mPTP opening and protects the rabbit heart from prolonged ischemia-reperfusion injury (1). Collectively, these studies have demonstrated the protective effect of TMZ when the kidney is exposed to warm ischemia (WI)-reperfusion. It was also shown that TMZ is efficient in protecting the liver from IRI in a rat model (10). These effects were well correlated with an inhibition of mitochondrial damage, since TMZ restored ATP synthesis, NAD(P)H levels, and mitochondrial membrane potential and generation of mitochondrial permeability transition (10). Altogether, these data outline the central role of mitochondria and the correlation between its damage during WI and cell dysfunction during reperfusion. However, data available from these reports are limited to the early time of reperfusion

(a few hours to a few days) and the long-term effects of TMZ remain to be clarified.

The present preclinical study was designed to study early and long-term effects of TMZ against different WI times followed by reperfusion, mimicking different clinical situations such as aortic and renal surgery. To clarify the impact of TMZ, we have focused on new pathophysiological factors that have recently emerged in IRI. Hypoxia-inducible factor 1 (HIF-1α) in acute hypoxic injury is known to upregulate factors that have been shown to be "cytoprotective." In addition, strategies that limit HIF prolyl-hydroxylation or HIF proteolysis may be powerful in improving IRI. Consequently, we have compared HIF expression in reperfused tissue exposed or not exposed to TMZ treatment. Acute tubular necrosis (ATN) is also characterized by a regeneration phase, which involves a sequence of events, including epithelial cell dedifferentiation and proliferation (2). Stathmin is an important molecule that is known to play a critical role in the process of mitosis and the regulation of the microtubule cytoskeleton. In ATN, recent reports have shown that stathmin is a marker of dedifferentiated, mitotically active epithelial cells that may contribute to tubular regeneration after ATN (44). Interestingly, in stathmin-deficient mice subjected to IRI, aberrant regulation of cell cycle progression, which impaired or at least delayed the process of tubular repair and recovery after acute renal injury, has been described (45). The other relevant aspect, the role of the inflammatory process in damaged kidneys, has been studied in in vitro and in vivo models, which have evidenced that inflammation plays a major role in the pathophysiology of ARF resulting from ischemia. Given that T lymphocytes are shown to be important pathogenic modulators in allo-antigen- independent injury to the kidney, leading to long-term dysfunction (5, 6), we have completed our experimental protocol with an analysis of cell populations involved in the inflammatory reaction within damaged tissue, adhesion molecule expression, and fibrosis development.

METHODS

Surgical procedures and experimental groups. Large white male pigs (INRA, J. C. Caritez, Le Magneraud, Surgères, France) were prepared as previously described (14). WI was induced by clamping the left renal pedicle for 45 (WI-45, $n = 7$), 60 (WI-60, $n = 8$), and 90 min (WI-90, $n = 8$) with a vascular nontraumatic clamp, followed by a right nephrectomy. TMZ was administered (5 mg/kg iv) 24 h before WI (WI-45-TMZ, $n = 8$, WI-60-TMZ, $n = 8$, and WI-90-TMZ, $n = 8$). These experimental groups were compared with the uninephrectomized group (UNX; $n = 8$, matched for weight, nephronic mass, and age) and the control group (sham-operated; $n = 6$, matched for weight and age). All experiments were carried out in accordance with the Guidelines of the French Agricultural Office and legislation governing animal studies. Animals were followed up at 16 wk after WI.

Functional parameters. Endogenous creatinine clearance (C_{Cr}; expressed in ml/min) and urinary proteins were measured as previously described (14). Pigs were placed in cages to allow specific 24-h urine collections. Plasma and urinary creatinine (C_r) was measured enzymatically (Jaffé method, rate blanked and compensated, Roche Diagnostic, Mannheim, Germany), and the glomerular filtration rate was calculated by determination of C_{cr} calculated using the following formula: urinary flow rate (UFR) $\times$ urinary C_r/plasma C_r. Urinary proteins were determined using a colorimetric method (Roche Diagnostic).

Supplementary animals were submitted to the same experimental conditions and killed at 3 h ($n = 2$) *day 1* ($n = 2$), *day 3* ($n = 2$), and *day 7* ($n = 2$) for TR-PCR and Western blot studies in renal tissue.

Real-time PCR using SYBR green for stathmin. Between *days 1* and *7*, stathmin mRNA in the cortex and outer medulla was measured to assess the influence of TMZ treatment on renal regeneration. Real-time quantitative PCR amplification reactions were carried out using the Smart Cycler detection system (Cepheid, Sunnyvale, CA) in a 25-μl volume. The reaction mixture consisted of 1$\times$ QuantiTect SYBR Green PCR Master Mix (Qiagen, Courtaboeuf, France) and an additional 0.5 mM MgCl$_2$, 0.5 and 1.25 U of Ampli*Taq* Gold DNA polymerase (Roche, Meylan, France), and 0.4 μM of each primer. One microliter of prepared cDNA template was added to each reaction. To quantify stathmin, 18S RNA was used as an internal control. The RT-PCR for stathmin and 18S rRNA were performed on the same cDNA samples in separate tubes. The primer sequences for PCR were as follows: stathmin (GenBank accession no. AY644720), forward 5′-CAGGTGAARGARCTNGARAACG-3′, reverse, 5′-ATTAGT-CAGCYTCNGTYTCRTCNGC-3′; and 18S rRNA forward, 5′-CGTCCCCGCCCCTTGCCTCT-3′, reverse 5′-GCTTTCGCTCTG-GTCCGTCTT-3′.

Western blotting. Pieces of snap-frozen kidney tissues (cortex and outer medulla) were disrupted in a mortar and then homogenized with a polytron at 0°C in Triton X-100 lysis buffer (50 mmol/l Tris, pH 7.6, 150 mmol/l NaCl, 1% Triton X-100, 0.1% SDS) containing 1% aprotinin, 2 mmol/l ϵ-aminocaproic acid, and 0.5 mmol/l phenylmethylsulfonyl fluoride. The homogenate was centrifuged at 2,000 *g* for 5 min. The supernatant was then centrifuged at 12,000 *g* for 5 min and retained. Protein concentrations were determined, and 50 μg of protein extracts, denatured in Laemmli buffer and separated on 12% SDS-PAGE, were electrotransferred to a nitrocellulose membrane. The membrane, blocked for 2 h at room temperature with TBS, 0.05% Tween 20, and 5% nonfat dry milk, was incubated overnight at 4°C with a 1:1,000-diluted rabbit anti-stathmin peptide antiserum against an amino acid sequence conserved across species as previously described (STC, Prof. A. Sobel, INSERM U.440, Paris, France) and with an 1:1,000-diluted HIF-1 (1:1,000, Novus Biologicals); an anti-rabbit antibody, conjugated to horseradish (Amersham Biosciences), was then used with a chemiluminescent technique to reveal the labeled bands (ECL kit; Amersham Biosciences). Immunoblotting of GAPDH was used to normalize the amounts of proteins loaded onto the SDS-PAGE (1:1,000; neoMarker, Fremont, CA). Image densito-

Table 1. *List of antibodies used*

Antibody	Ref. No.	Origin	Isotype	Specificity
Mouse anti-human CD106	MCA907B	Serotec products (Oxford, UK)	IgG1	VCAM-I
Mouse anti-porcine MHC class II	MCA1335	Serotec products	IgG2b	MHC class II
Mouse anti-porcine macrophage and monocyte	MCA1218	Serotec products	IgG2b	Monocytes/macrophages
Mouse anti-porcine CD4$^+$	MCA1749	Serotec products	IgG2b	T helper lymphocytes
Mouse anti-porcine CD8$^+$	MCA1223	Serotec products	IgG2a	T cytotoxic/suppressor lymphocytes

The anti-human antibody used cross-reacted with the pig species.

metric analysis of the immunoreactive protein bands was performed using OptiQuant image-analysis software (Packard BioScience, Meriden, CT).

Histopathological studies. Biopsies of tissue samples from the deep cortex-outer medulla region were collected at *days 1*, *3*, *5*, *7*, and *14*, and at 4–5, 10–12, and 16 wk after every WI followed by the reperfusion process. Conventional stains were applied (hematoxylin and eosin, periodic acid-Schiff). Different histological parameters (tubular necrosis, brush-border integrity, and intratubular detachment) were studied. Histological lesions were expressed in a percentage of kidney samples using a previously described semiquantitative scale (13): 0, no abnormality; 1, mild lesions affecting <10% of kidney samples; 2, lesions affecting 10–25% of kidney samples; 3, lesions affecting 25–50% of kidney samples; 4, lesions affecting 50–75%; and 5, lesions affecting >75% of kidney samples. Mitochondrial integrity was also measured using electromicroscopy. Tubulointerstitial injury was defined as inflammatory cell infiltrates, tubular atrophy,

or interstitial fibrosis. To estimate the level of tubulointerstitial fibrosis, tissue sections were also labeled with Picro Sirius for collagen identification (collagen I and III) as recommended (19). The amount of interstitial fibrosis was determined in Picro Sirius-stained sections by a semiquantitative imaging technique. Image analysis was performed by either a technician or a pathologist blinded to the clinical source of the sample. The slides were examined with a microscope, and the images were acquired using a ×40 objective. The percentage of Picro Sirius-stained surface was determined by a computer-aided image-analysis program. In each representative slide, staining in renal tissue was semiautomatically quantified in 15 fields by the computer program in each experimental condition and expressed as percentage of the total surface area examined. Tubular atrophy was semiquantitatively scored on a scale of 0–4+ by two pathologists blinded to the experimental conditions (0, normal; 1, small changes affecting 5–10%; 2, changes affecting 10–25% of specimen area; 3, changes affecting 25–50% of specimen area; 4, changes affect-
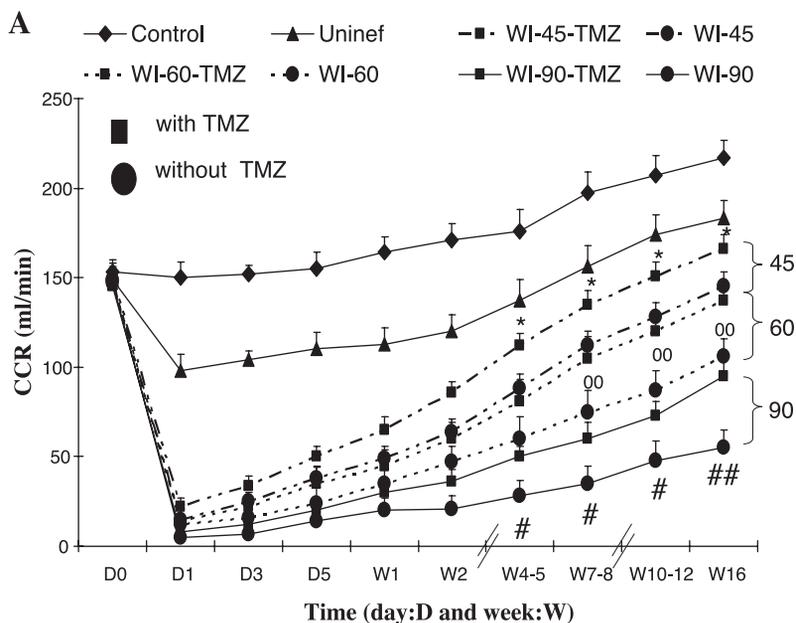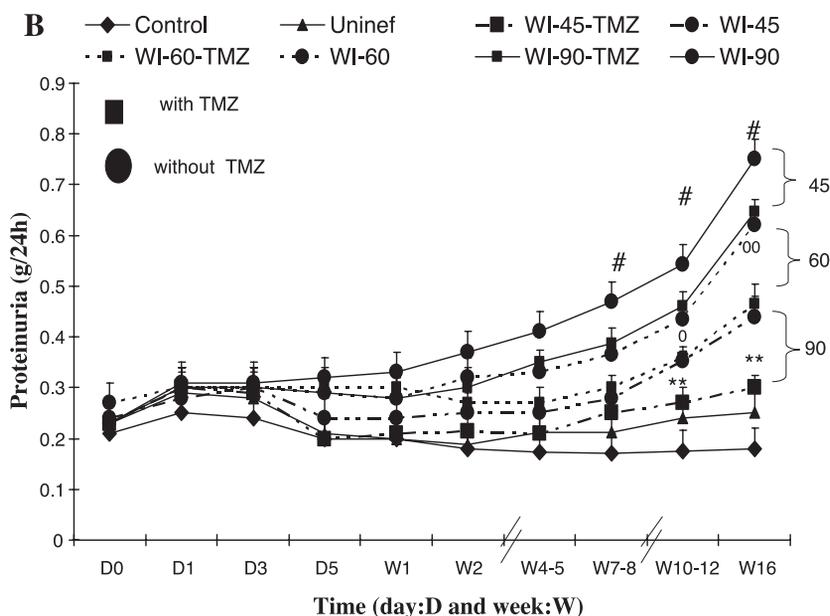

Fig. 1. Influence of trimetazidine (TMZ) on warm ischemia (WI) time on creatinine clearance (*A*) and protein excretion (*B*). Renal function was measured in the different experimental groups after different WI times and compared with control group and uninephrectomized group. Values are means ± SE. *$P < 0.05$, **$P < 0.01$ WI-45 vs. WI-45-TMZ. °$P < 0.05$,°°$P < 0.01$ WI-60 vs. WI-60-TMZ. #$P < 0.05$ WI-90 vs. WI-90-TMZ.

ing 50–75% of specimen area; and 5, changes affecting 75–100% of specimen area).

Immunohistochemical studies. Frozen and paraffin-embedded kidney biopsy sections (5 μm) were processed for indirect immunohistochemistry using several mouse monoclonal antibodies (mAbs; dilution 1:20) as previously described (13) by using the antibodies listed in Table 1. Indirect immunofluorescence was performed by using an anti-human VCAM-1 antibody (see Table 1). All sections were examined under blind conditions and photographed. The degree of MHC class II and VCAM-1 staining was semiquantitatively estimated (0, no staining to 4+, dense) and the number of MCA1218-, CD4$^+$-, CD8$^+$-labeled cells per surface area ($10^4/\mu m^2$) was counted in five different tissue sections for each of the experimental conditions as described (13, 14).

Statistical analysis. Quantitative parameters are presented as means ± SE and qualitative parameters as percentages. Statistical differences between groups were calculated using an unpaired *t*-test or analysis of variance and the Student-Newman-Keuls or the Kruskal-Wallis test for multiple comparison analyses. A *P* value < 0.05 was considered to be significant.

RESULTS

Evolution of long-term renal functions and survival after varying intervals of WI with and without TMZ. Several animals from nontreated groups died in postoperative days due to the intensity of WI. Four animals in the WI-90 group died between postoperative *days 8* and *10* and two in the WI-60 group between *days 9* and *12*. All these animals were autopsied to check for surgical or anastomotic problems. Survival was 100% in sham-operated, UNX, W-I45, WI-60-TMZ, and WI-90-TMZ groups, respectively. The effects of 10 and 30 min of WI were evident, and no detectable effect of TMZ was observed compared with nontreated pigs (data not shown). Consequently, intervals of 10 and 30 min of WI did not cause substantial damage to pig kidney, which is an experimental condition very close to the clinical one. Renal functional data are shown in Fig. 1, *A* and *B*. During the first week, C_{Cr} was reduced in both treated and nontreated groups (WI-45–WI-90) compared with control and sham-operated groups (Fig. 1*A*). However, differences were significant ($P < 0.05$, $P < 0.01$) between TMZ-treated and non-treated groups for 45 min of WI (W2 and W16), for 60 min of WI (W7–8 to W16), and for 90 min of WI (between W4–5 and W16): TMZ induced a lesser C_{Cr} decrease. Progressive proteinuria developed again after ~6–8 wk (Fig. 1*B*). The highest levels of proteinuria were

detected in the WI-60 and particularly in WI-90 groups. When TMZ was administered before WI, proteinuria was reduced for WI of 45, 60, and 90 min, WI-60-TMZ, and WI-90-TMZ. As assessed in the two tests (C_{Cr} and proteinuria), TMZ (5 mg/kg iv) administered 24 h before WI was always effective, but their improvements were only partial.

Evolution of cellular integrity of postreperfused kidneys after varying intervals of WI with and without TMZ. Histological analysis of biopsy samples from WI kidneys revealed some differences in the cellular integrity after 40 min of reperfusion and at *day 7* postreperfusion. TMZ treatment in WI-30 groups exhibited a very low level of difference (data not shown). Kidneys from the WI-45 group exhibited reduced damage compared with WI-60 and particularly WI-90 groups (Table 2). The degree of initial acute proximal tubule cell injury appeared closely related to the duration of WI, particularly after 60 min of WI (Table 2). The WI-60 and WI-90 groups exhibited an intense proximal tubule necrosis with a significant loss of brush border and proteinacious cast. TMZ reduced the injury score after WI-45, and particularly after 60 and 90 min of WI. The protective effect of TMZ was more pronounced on brush-border integrity and mitochondria (Table 2 and Fig. 2). Interestingly, TMZ-pretreated groups presented a more reduced injury score at *day 7* compared with WI groups particularly after 60 and 90 min of WI, which is related to the repair process.

Effect of varying intervals of renal ischemia with and without TMZ on stathmin mRNA and stathmin and HIF-1α protein expression in pig kidneys. Our results indicate that the expression of stathmin mRNA increases in all IRI samples and that the greatest increase was found in the RNA extracted from kidneys subjected to TMZ treatment (Fig. 3) and especially in pig kidneys treated with TMZ after 3-h reperfusion. At *day 7*, stathmin mRNA was significantly increased in groups without TMZ compared with TMZ-treated groups, suggesting that the process of tubular repair and recovery after acute renal injury was not delayed in TMZ-treated groups. Stathmin protein increased and reached its peak levels by 72 h after the induction in ischemia. Stathmin expression was increased in TMZ-perfused pig kidneys at *day 1* (Fig. 4*A*). At *day 7*, stathmin expression decreased in experimental groups with TMZ (particularly WI-45-TMZ and WI-60-TMZ groups) compared with nontreated groups (Fig. 4, *A* and *B*, *bottom*). HIF-1α was not

Table 2. *Degree of proximal tubule cell lesions and mitochondrial damage after different periods of warm ischemia*

Injury Type/Reperfusion Time	WI-45-TMZ/WI-45	WI-60-TMZ/WI-60	WI-90-TMZ/WI-90
Brush-border integrity			
30–45 min	3.6±0.2/3.4±0.2	3.0±0.3/2.7±0.2	2.5±0.2/2.2±0.2
day 7	4.2±0.2/3.6±0.2*	3.7±0.2/3.1±0.1†	3.3±0.2/2.5±0.2‡
Tubular necrosis			
30–45 min	2.4±0.2/2.7±0.3	2.9±0.3/3.2±0.2	3.5±0.2/3.8±0.2
day 7	1.1±0.1/1.6±0.2*	2.0±0.2/2.5±0.2†	2.3±0.2/3.0±0.2‡
Mitochondrial injury			
30–45 min	2.1±0.2/2.4±0.2	2.7±0.2/3.5±0.2	3.6±0.3/4.1±0.3
day 7	1.2±0.2/1.8±0.2*	1.7±0.3/2.3±0.2†	2.5±0.2/3.2±0.2‡

Values are means ± SE for all parameters analyzed. The histological lesions from early (30–40 min) and *day 7* post-warm ischemia (WI) were evaluated and given as a semiquantitative score (METHODS). TMZ, trimetazidine. Brush-border integrity, tubular necrosis (characterized by swollen cells with granular cytoplasm and mitotic figures), and mitochondrial injury (characterized by mitochondrial swelling, rupture of outer and inner membranes, and leakage of mitochondrial matrix into the cytoplasm) were examined in light and electron microscopic studies, respectively. *$P < 0.05$ WI-45 vs. WI-45-TMZ. †$P < 0.05$ WI-60 vs. WI-60-TMZ. ‡$P < 0.05$ WI-90 vs. WI-90-TMZ.

Fig. 2. *Top* and *bottom*: effect of WI on brush-border and mitochondrial integrity, respectively, in postreperfused kidneys. WI-45 and WI-TMZ-45, WI-60 and WI-TMZ-60, and WI-90 and WI-TMZ-90 (45, 60, and 90 min of WI, respectively) kidney samples are presented after reperfusion and compared with control and uninephrectomized groups. bb, Brush border; tl, tubular lumen. Brush-border integrity and mitochondrial density in different groups are represented by arrows. mt, Mitochondria. Mitochondria density was reduced in WI-60 and particularly WI-90. Biopsy samples from WI-30 are not presented because the absence of damage is sufficiently remarkable. *Middle*: effect of WI on tissue integrity in postreperfused kidneys. WI-45 and WI-TMZ-45, WI-60 and WI-TMZ-60, and WI-90 and WI-TMZ-90 kidney samples are presented after reperfusion. WI-30 biopsy samples are not presented because the absence of damage is sufficiently remarkable. Brush-border preservation is represented by arrows.
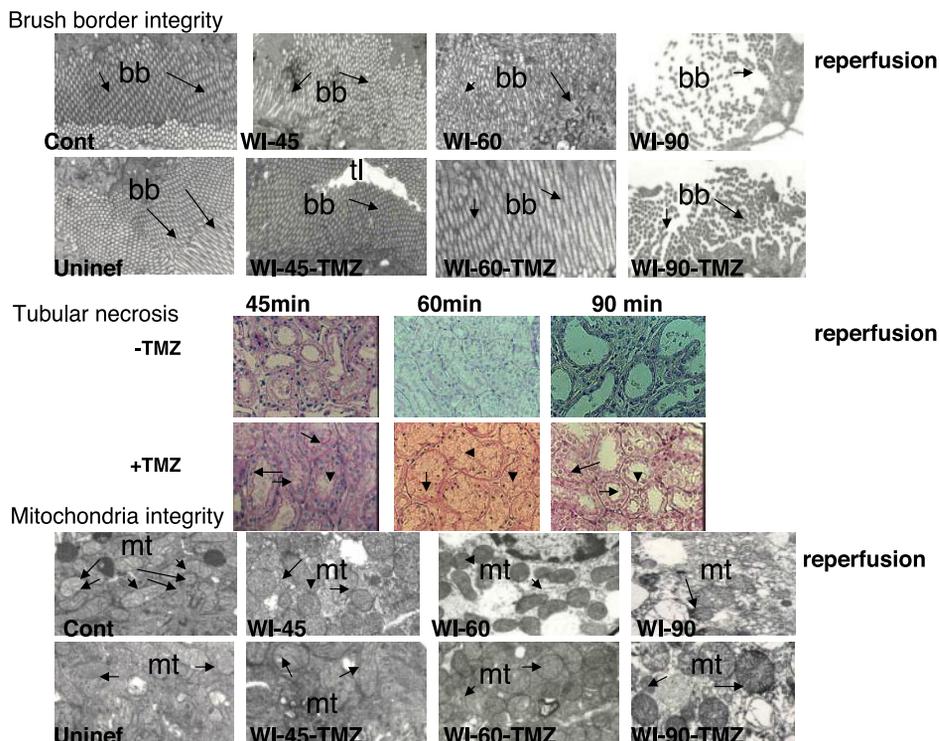

detected at *day 0* (basal level). The HIF-1α increase occurred within 3 h after reperfusion in TMZ-treated groups and in the WI-45 group and peaked at *day 7*. In turn, the HIF-1α protein increase was delayed in groups without TMZ pretreatment (Fig. 4*B*, *bottom*). This data support indicated that the process of tubular repair and recovery after acute renal injury was delayed in non-TMZ-treated groups. In addition, the production of HIF-1α, which was correlated with the excretion of cytoprotective factors such as VEGF or erythropoietin, was delayed in non-TMZ-treated kidneys.

Effect of varying intervals of renal ischemia with and without TMZ on MHC class II expression in pig kidneys. The expression of MHC class II molecules was analyzed after WI (Table 3 and Fig. 5). The topology of immunostaining mainly involved the peritubular capillary endothelial cells and sur-rounding inflammatory cells. The WI-60 and WI-90 groups exhibited a more diffuse and intense immunolabeling in these cells. Proximal tubule, thick ascending limb of loop of Henle, and collecting duct epithelial cells were always negative. Rarefied MHC class II vascular endothelial cells were observed in the W45 groups. TMZ reduced MHC class II expression in all WI groups and particularly in the WI-60 and WI-90 groups.

Effect of WI on cellular infiltration and VCAM-1 expression in pig kidneys after various WI periods with and without TMZ. In accordance with previous studies, the major inflammatory cell population detected by immunohistochemical studies was CD4$^+$ T lymphocytes. No infiltrating cell was detected in control, UNX, and WI-10 (data not shown). Almost no infiltrating CD4$^+$ and CD8$^+$ cells were detected in the remaining kidney from the WI30 group (data not shown). In contrast, the

Fig. 3. Expression of stathmin mRNA after various durations of ischemia followed by reperfusion in cortex and outer medulla. The stathmin mRNAs were standardized against 18S rRNA and expressed as ratios of the value of standardized stathmin in sham-operated kidneys as described in METHODS. Values are means $\pm$ SE from 3 independent experiments. *$P < 0.05$, **$P < 0.01$ vs. sham-operated and control groups (0 h).
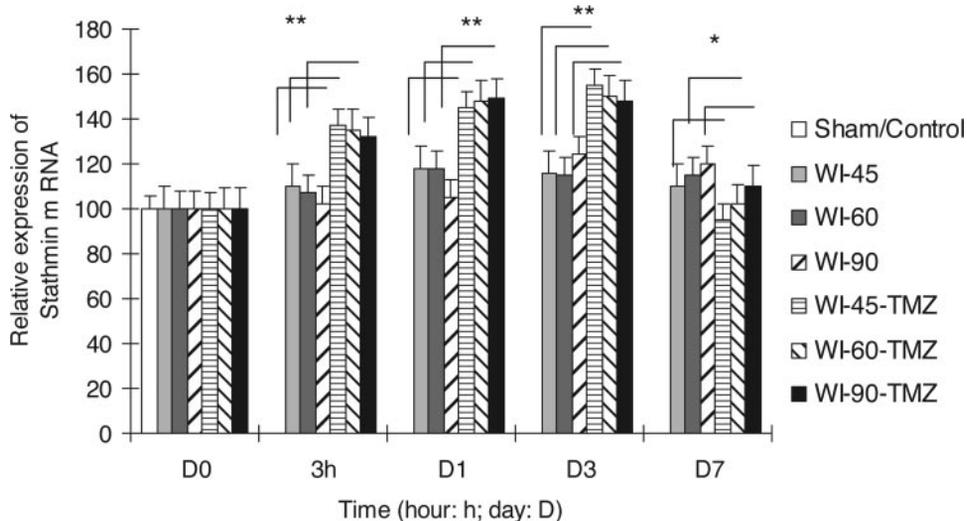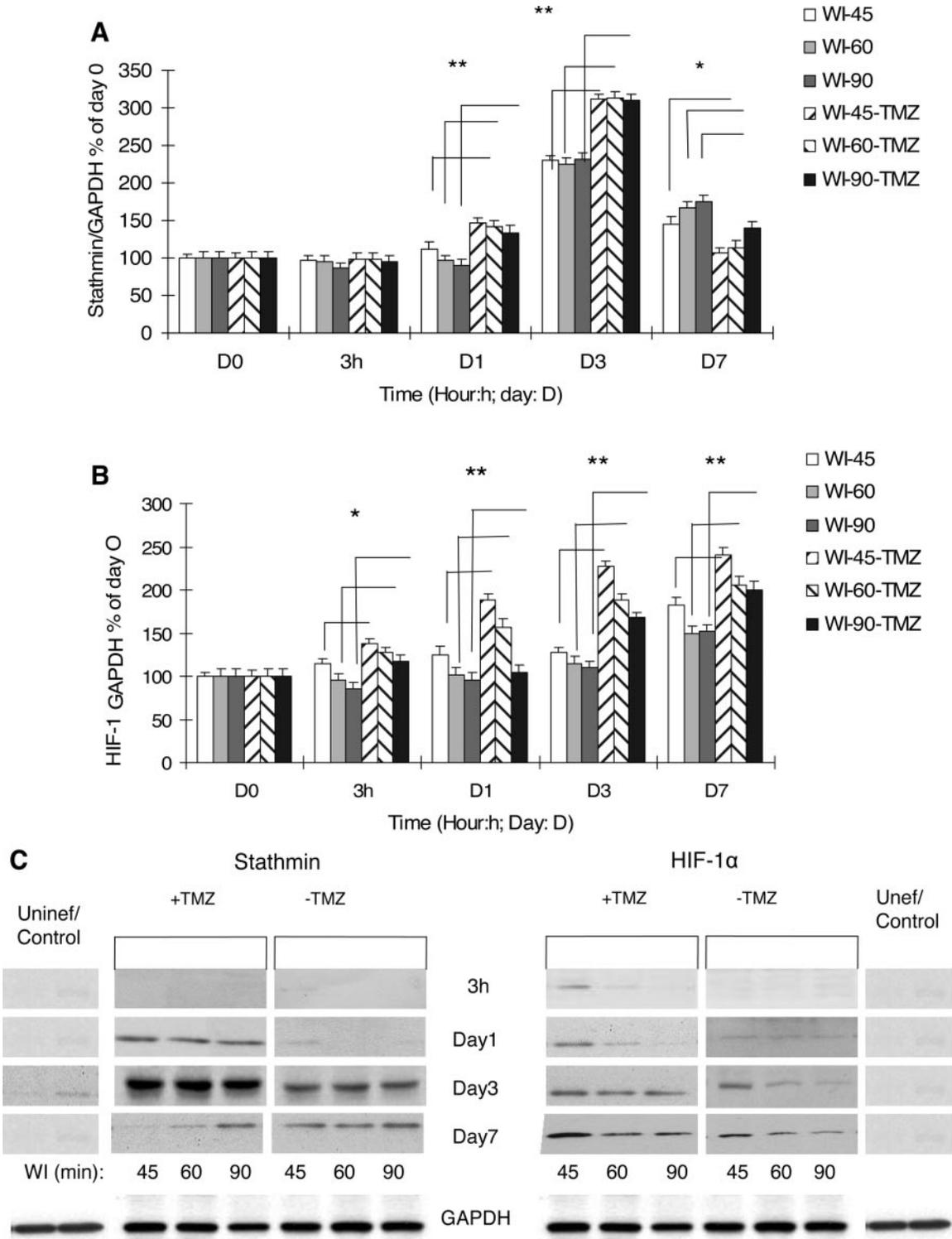
Fig. 4. Western blot analysis of stathmin and hypoxia-inducible factor-1 (HIF-1α). *A* and *B*: expression of stathmin and HIF-1α, respectively, was examined by Western blotting in cortex and outer medulla at *days 0*, *3*, and *7* after reperfusion. *C*: representative immunoblots for stathmin, HIF-1α, and control actin after various durations of ischemia (45, 60, and 90 min) followed by reperfusion and stathmin and HIF-1α expression in normal kidney (control) and uninephrectomized animals. Induction of stathmin and HIF-1α was observed at 72 h of reperfusion, particularly in the outer medulla in TMZ-treated groups, and this induction was delayed in no TMZ-treated groups. Values are means ± SE from 3 independent experiments. *$P < 0.05$ TMZ-treated groups vs. no TMZ-treated group and sham-operated and uninephrectomized groups (0 h). **$P < 0.01$ TMZ-treated groups vs. no TMZ-treated group and sham-operated and control groups (0 h).

Table 3. *Semiquantitative analysis of MHC class II expression*

	Week 1	Week 2	Weeks 4–6	Weeks 8–12	Week 16
	WI-45/WI-45-TMZ				
Endothelial cells	++ to +++/+ to ++	++/+	++/+	++/+	++/+
Tubular cells	0 to +/+	0/0 to +	0/0 to +	0/0	0
Inflammatory cells	++ to +++/++	++/+	++/+	++/+	++/+
	WI-60/WI-60-TMZ				
Endothelial cells	+++/++	+++/++	+++/++	++/+	++/+
Tubular cells	+/0	+/0	+/0 to +	+/0 to +	0/0 to +
Inflammatory cells	+++/++	+++/+++	+++/+++	+++/++	+++/++
	WI-90/WI-90-TMZ				
Endothelial cells	+++/++	+++/++	+++/++	+++/++	+++/++
Tubular cells	+/0	+/0	+/0	+/0	+/0
Inflammatory cells	+++/++	+++/++	+++/++	+++/++	+++/++

Semiquantitative graded score of the immunostaining was used (0, no staining to 4+, dense). For details, see METHODS.

number of CD4$^+$ cells increased proportionally to the WI periods for 4 wk after reperfusion in the WI-45 and particularly WI-60 and WI-90 groups (Fig. 6*A*). After 4 wk, CD4$^+$ cells slowed to a plateau up to 16 wk following reperfusion in the WI-45 group and slightly increased in the WI-60 and WI-90 groups. The number of CD8$^+$ cells increased also with the WI time, particularly in the WI-60 and WI-90 groups (Fig. 6*B*). However, the number of CD8$^+$ cells was much lower and gradually increased with longer WI periods. The number of macrophages/monocytes increased from *day 1* to *days 5–7* according to WI time and decreased between *day 7* and *week 2*, particularly for the WI-45 group. In the WI-60 and WI-90 groups, monocytes/macrophages increased between *day 1* and *day 7*, then slightly decreased between *day 7* and *day 14*, increased again, and then remained unchanged after 10-wk follow-up (Fig. 6*C*). Unlike cold-ischemic injury, the biphasic process of inflammatory cell infiltration in interstitial areas was less prominent. TMZ reduced the inflammatory response in all groups and particularly in the WI-60 and WI-90 groups. VCAM-1 demonstrated a mild staining in tubulointerstitial areas in the WI-45 group. VCAM-1 expression increased with WI times in the WI-60 and WI-90 groups. These groups
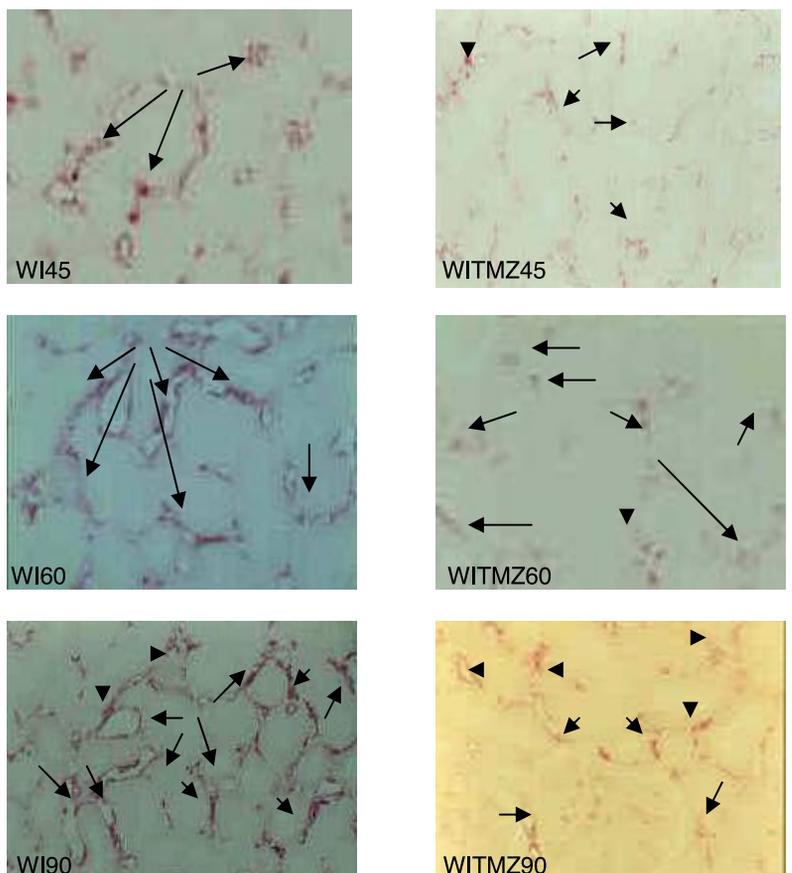

Fig. 5. Effect of WI time on MHC class II distribution in postreperfused kidneys. Biopsy samples were processed for immunohistochemistry using MCA 1335 anti-porcine MHC class II-DQ. The most intense staining (arrows) was noted in WI-45, WI-60, and WI-90 (*left*) compared with WI-TMZ-45, WI-TMZ-60, and WI-TMZ-90 (*right*). Semiquantitative graded score of immunostaining was used (0: no staining to 4+: dense).

exhibited a more intense VCAM-1 staining in tubular, peritubular capillary, and inflammatory cells (Fig. 7 and Table 4). TMZ-treated groups exhibited a reduced expression of VCAM-1 during the 18-wk follow-up.

Effect of WI on the onset of interstitial fibrosis after various WI periods with and without TMZ. The evolution of interstitial fibrosis is presented in Fig. 8*A* and *B1* to *B6*. In our hands, fibrosis was correlated with the duration of WI, particularly
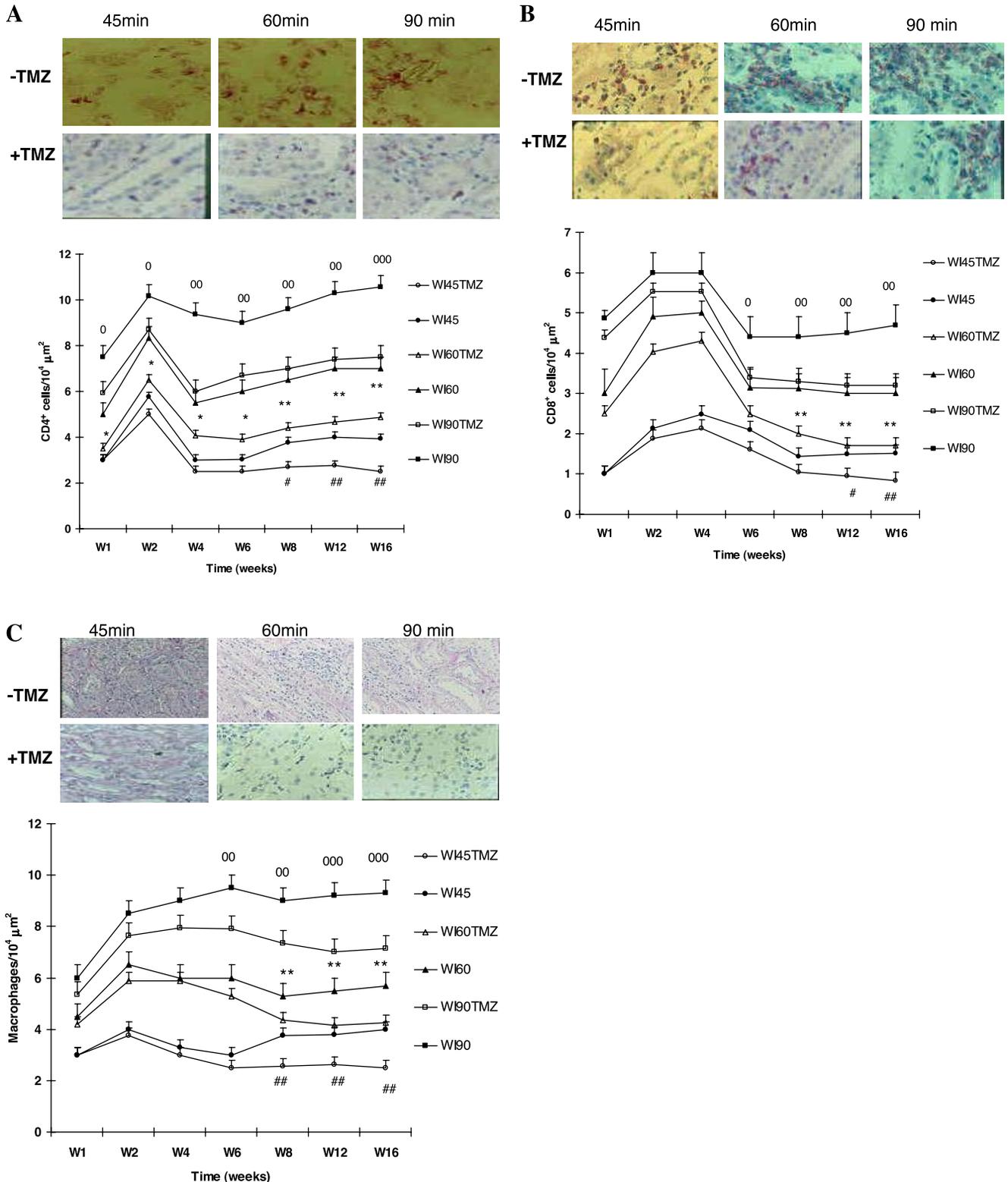

Fig. 6. Effect of WI time inflammation in postreperfused kidney: *A*: CD4$^+$ cells. *B*: CD8$^+$ cells. *C*: monocytes/macrophages. The number of positively stained per surface area was counted in biopsy samples from experimental groups. Values are means ± SE from 8–12 separate determinations. *$P < 0.05$, **$P < 0.01$ WI-45 vs. WI-45-TMZ. °$P < 0.05$, °°$P < 0.01$ WI-60 vs. WI-60-TMZ. #$P < 0.05$ WI-90 vs. WI-90-TMZ.

after 60 min and 90 min of WI (Fig. 7, *A* and *C*). The percentage of interstitial fibrosis area was also related to the progression of CCR as observed to the WI-45 group compared with WI-60 and WI-90 groups. These changes were accompanied by an atrophy of the surrounding tubules and significant interstitial fibrosis. The lesions in WI-60 and WI-90 groups exhibited a focal-radial character and are characterized by patchy destruction of renal structures (tubuli, glomeruli and vessels). Within kidneys from TMZ-treated groups, fibrosis development was reduced (Fig. 8*A* and *B4* to *B6*).

DISCUSSION

ARF caused by IRI is among the major causes of morbidity in hospitalized patients and indicates poor prognosis in patients with multisystem organ failure. The reduction in regional blood flow to the outer medulla occurring during IRI is more pronounced than that to the cortical capillaries in the postischemic kidney (36). In the present study, we have demonstrated a strong correlation between C_{Cr} evolution and WI times as previously suggested (26). TMZ improved C_{Cr} in all groups, particularly in WI-90-TMZ 2 wk after reperfusion. These functional data were associated with the improvement of mitochondrial function itself. This was clearly observed particularly at *day 7* compared with the one observed after 40 min of reperfusion. Recently, it was also demonstrated that TMZ improved mitochondrial functions of the myocardium subjected to several I/R in an experimental canine model (25). The mitochondrial morphological changes to "rod-like" seen in the TMZ-treated group indicate that mitochondria require a larger membrane surface area to produce ATP. In addition, TMZ in this model also increased mitochondrial turnover. Recently, TMZ was suggested to inhibit mitochondrial permeability transition pores and prevent lethal IRI after coronary artery occlusion (1). These data demonstrate that TMZ could limit apoptotic cardiomyocyte death and support recent findings by Yin et al. (40), who showed a similar antiapoptotic effect in cultured astrocytes subjected to hypoxia-reoxygenation. Collectively, these data suggest that TMZ protects mitochondria from IRI.

As to the effect of TMZ on renal regeneration, this drug improved the repair process level, as supported by its effect on stathmin expression. Stathmin, an 18-kDa protein, is expressed in cells that have reentered the cell cycle (30). Stathmin expression was found to be positively correlated with cellular proliferation in different cell lines (31). Interestingly, stathmin expression was shown to decrease on induction of differentiation and cessation of proliferation in undifferentiated cell lines. It regulates microtubule dynamics by promoting depolymerization of microtubules and/or preventing polymerization of tubulin heterodimers and can be regulated by phosphorylation. Recent studies have demonstrated that stathmin can have two distinct activities. Stathmin is capable of binding both polymerized and unpolymerized tubulin and can prevent polymerization of heterodimers under some conditions and/or promote depolymerization of microtubules under others (for a review, see Ref. 31). Previous studies have demonstrated that the expression of stathmin increases in the proximal tubules of kidneys subjected to IRI (44). Stathmin was expressed by dedifferentiated and actively proliferating proximal tubule cells in the corticomedullary junction and in the S3 segment of the proximal tubule (39). Recently, it was suggested that in stathmin-deficient mice subjected to IRI, the aberrant regulation of cell cycle progression impairs or at least delays the process of tubular repair and recovery after acute renal injury (45). In our study, the protective effect of TMZ in renal tissue of pretreated groups was correlated with an earlier and higher expression of stathmin than in renal tissue without TMZ treatment. This effect on stathmin, which is involved in the regulation of mitosis and proposed to be a relay integrating diverse intracellular signaling pathways controlling cell proliferation, differentiation, and functions, could be related to a recently suggested effect against dephosphorylation of nucleotides during ischemia (8). In addition, these results suggest that stathmin is a critical protein in the regulation of cell mitosis in damaged

A: WI-45, **B**: WI-60, **C**: WI-90, **D**: WI-45-TMZ,
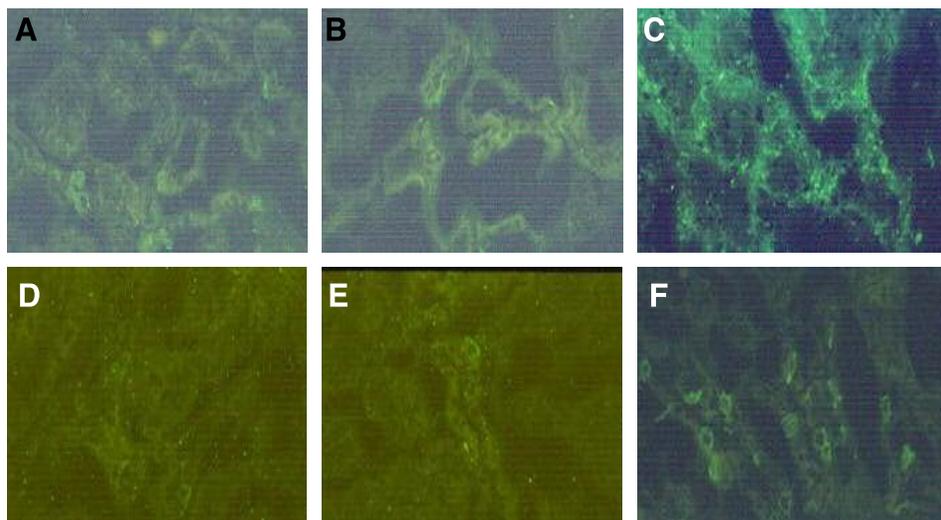**E**: WI-60-TMZ and **F**: WI-90-TMZ

Fig. 7. Effect of WI on VCAM-1 expression in reperfused kidneys: semiquantitative graded score of the immunostaining provided by the anti-VCAM1 mAb (0: no staining to 4+: dense). *A*: WI-45. *B*: WI-60. *C*: WI-90. *D*: WI-45-TMZ. *E*: WI-60-TMZ. *F*: WI-90-TMZ.

Table 4. *Semiquantitative analysis of VCAM-1 expression*

	Week 1	Week 2	Weeks 4–6	Weeks 8–12	Week 16
WI-45/WI-45-TMZ	0 to +/0	+/0 to +	+/0 to +	+/0 to +	+/0 to +
WI-60/WI-60-TMZ	+/0 to +	+ to ++/+	++/+	++/+	++/+
WI-90/WI-90-TMZ	++/+	++/+	+++/+ to ++	+++/++	+++/++

Semiquantitative graded score of immunostaining was used (0, no staining to 4+, dense). For details, see METHODS.

tissue. Interestingly, cells in kidneys of TMZ-pretreated groups were able to express stathmin more rapidly and strongly than cells in kidney of TMZ-unpretreated groups, where stathmin expression is delayed. On the other hand, the persistence of stathmin expression within kidneys from untreated animals could be related to prolonged cell stress. Such results are in accordance with previous data which have demonstrated that stathmin mRNA and protein reached a peak at 24-h posthepatectomy, then decreased until 96 h after hepatectomy (21). Taken together, these results reveal an innovative aspect of the protective role of TMZ in regulatory pathways of cell proliferation and differentiation during regeneration.

Regarding the effect of TMZ on HIF-1α, its expression was delayed in nontreated groups particularly after 90 min of WI. As a global regulator of hypoxic adaptation, HIF is involved in the regulation of mitochondrial signaling, hypoxic cell death, and recovery from IRI. HIF-1 is known to upregulate factors that have been shown to be cytoprotective. TMZ is involved in an earlier and more prolonged HIF-1α expression correlated with limitation of damage. The response of kidneys acutely damaged by ischemia or toxins is dominated by epithelial destruction and regeneration. Recent data have suggested that a reduction in the peritubular capillary density after ARF results in persistent reduction of renal P_{O_2} and that hypoxia may play an important role in the progression of chronic disease after ARF (6). In our model, the influence on renal recovery with a protective drug such as TMZ was efficient in delaying fibrosis development within tubulointerstitial tissue. Limitation of fibrosis was correlated with increases in C_{Cr} and reduction of proteinuria. Renal injury associated with IRI results from a dynamic process involving vascular network and tubules in a complex intereaction. Our data support previous findings on the counteracting role of TMZ in fibrosis development in different diseases. In a rat model of alkali burns of the esophagus, TMZ reduced the degree of fibrosis and limited histopathological damage (2). Given that a single episode of renal IRI is associated with increased chronic allograft nephropathy, which decreased long-term allograft nephropathic function, TMZ could be useful in the limitation of renal damage.

The other important finding was the impact of a single injection of TMZ 24 h before WI on inflammation processes. Recent years have seen the emergence of the role of inflammation in IRI. Leukocyte adhesion/infiltration and endothelial cell activation in response to IRI is a well-known phenomenon (3, 17, 41). In the current study, we have studied the late phase of inflammation. TMZ modulated monocyte/macrophage infiltration, which served at this late phase as a crucial interface between the innate and adaptative immune systems. T lymphocytes were also reduced by TMZ. Evidence from different laboratories supports a role for T cells as modulators of renal IRI, particularly in rodent models (for a review, see Ref. 5).

Using specific antibodies for inflammatory cells, the limitation of WI's deleterious effects by TMZ was correlated with the limitation of inflammation process after 45, 60, and particularly 90 min of WI. This effect could be related to an effect of TMZ
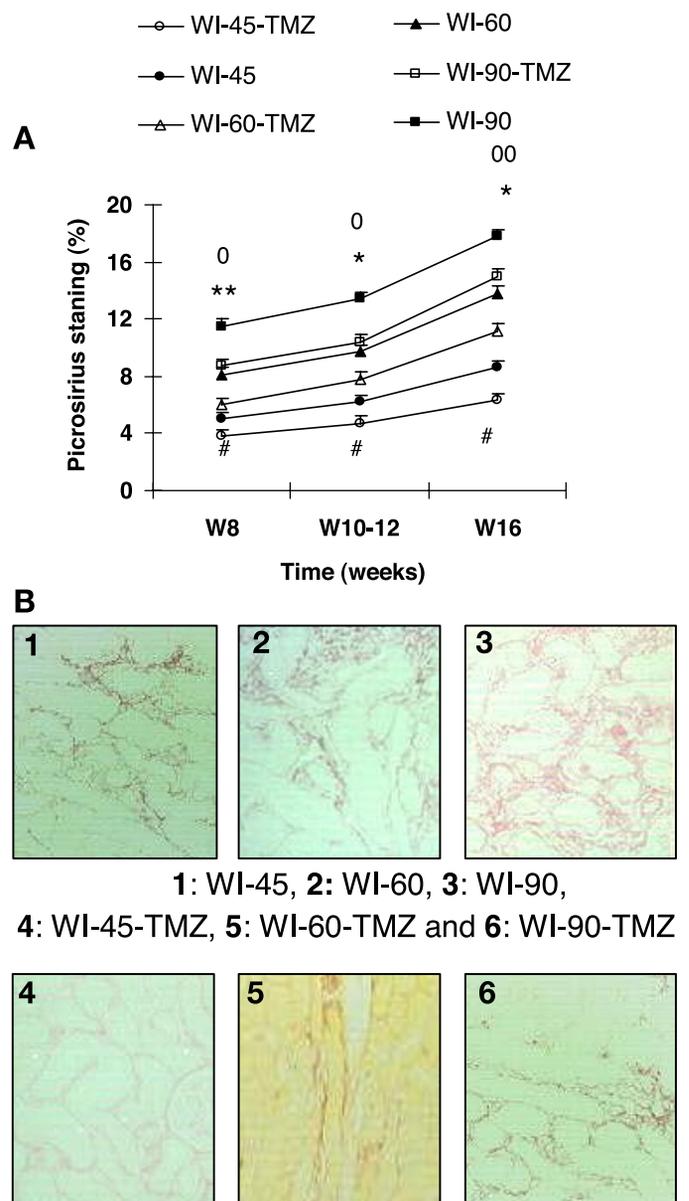

Fig. 8. Influence of WI on the onset of tubulointerstitial fibrosis. *A*: percentage of kidney areas displaying interstitial fibrosis stained with Picro Sirius was measured over several weeks following WI within kidneys between W8 and W16. *Bottom*: tubulointerstitial fibrosis determined using Picro Sirius red coloration at W16. Values are means ± SE. *$P < 0.05$, **$P < 0.01$ WI-45 vs. WI-45-TMZ. °$P < 0.05$. °°$P < 0.01$ WI-60 vs. WI-60-TMZ. #$P < 0.05$ WI-90 vs. WI-90-TMZ.

on IRI. In addition, ROS, generated during IRI, can also activate T cells (5, 42), and the role of TMZ against ROS production and mitochondrial damage could indirectly explain this effect (24, 38). Otherwise, TMZ reduced VCAM-1 expression, which could also participate in the limitation of inflammation via endothelial cells. VCAM-1 is transcriptionally induced on endothelial cells, and its engagement induces a signal in the endothelial cells that trigger changes in shape and allow leukocyte emigration. TMZ treatment influenced MHC class II expression. The expression of MHC class II antigens by the injured tubular epithelium, picked up by and presented by recruited dendritic cells to CD4$^+$ T cells, represents the auto-reactive cellular immunity important in the discrimination between self and nonself (7). These data indicated that when ischemic damage was severe, there was a progressive loss of tolerance to parenchymal self, inducing a persistent immune response (14, 29). This effect paralleled the fibrosis development within damaged tissue and indicated that the protective effect of TMZ is a global effect, which improved the regeneration of tissue and limitation of the long-term deleterious effect of IRI.

Consequently, the interest of TMZ in this model was supported by its role in the early and late phases of IRI. We have previously demonstrated the positive effect of TMZ in cold preservation (14–16). This effect was also remarkable in the WI pig kidney model, suggesting that TMZ could be useful in clinical transplantation where the permanent shortage of organs had led to attempts to expand the donor pool. In addition, our model allows designing a study with a long-term follow-up compared with most experimental studies, which focused on a short-term effect in the first days following an ischemic insult. TMZ could be particularly efficient in "controlled donors" (type III and IV from the Maastricht group) as an early single perfusion could limit fibrosis development (4, 16). It would be useful to address the best regimen of TMZ to be used and to check whether sequential administration to the recipient of the graft could restore renal function.

REFERENCES

1. **Argaud L, Gomez L, Gateau-Roesch O, Couture-Lepetit E, Loufouat J, Robert D, Ovize M.** Trimetazidine inhibits mitochondrial permeability transition pore opening and prevents lethal ischemia-reperfusion injury. *J Mol Cell Cardiol* 39: 893–899, 2005.
2. **Basile DP, Donohoe DL, Roethe K, Mattson DL.** Chronic renal hypoxia after acute ischemic injury: effects of L-arginine on hypoxia and secondary damage. *Am J Physiol Renal Physiol* 284: F338–F348, 2003.
3. **Bonventre JV, Weinberg JM.** Recent advances in the pathophysiology of ischemic acute renal failure. *J Am Soc Nephrol* 14: 2199–2210, 2003.
4. **Brook NR, Waller JR, Nicholson ML.** Nonheart-beating kidney donation: current practice and future developments. *Kidney Int* 63: 1516–1529, 2003.
5. **Burne-Taney MJ, Rabb H.** The role of adhesion molecules and T cells in ischemic renal injury. *Curr Opin Nephrol Hypertens* 12: 86–90, 2003.
6. **Burne-Taney MJ, Yokota N, Rabb H.** Persistent renal and extrarenal immune changes after severe ischemic injury. *Kidney Int* 67: 1001–1009, 2005.
7. **Chaudhri G, Clark IA, Hunt NH, Cowden WB, Ceredig R.** Effect of antioxidants on primary alloantigen-induced T cell activation and proliferation. *J Immunol* 137: 2648–2652, 1986.
8. **Domanski L, Sulikowski T, Safranov K, Pawlik A, Olszewska M, Chlubek D, Urasinska E, Ciechanowski K.** Effect of trimetazidine on the nucleotide profile in rat kidney with ischemia-reperfusion injury. *Eur J Pharm Sci* 27: 320–327, 2006.
9. **El Banani H, Bernard M, Baetz D, Cabanes E, Cozzone KB, Lucien A, Feuvray D.** Changes in intracellular sodium and pH during ischemia-reperfusion are attenuated by trimetazidine. Comparison between low- and zero-flow ischemia. *Cardiovasc Res* 47: 688–696, 2000.
10. **Elimadi A, Settaf A, Morin D, Sapena R, Lamchouri F, Cherrah Y, Tillement JP.** Trimetazidine counteracts the hepatic injury associated with ischemia-reperfusion by preserving mitochondrial function. *J Pharmacol Exp Ther* 286: 23–28, 1998.
11. **Faure JP, Baumert H, Han Z, Goujon JM, Favreau F, Dutheil D, Petit I, Barriere M, Tallineau C, Tillement JP, Carretier M, Mauco G, Papadopoulos V, Hauet T.** Evidence for a protective role of trimetazidine during cold ischemia: targeting inflammation and nephron mass. *Biochem Pharmacol* 66: 2241–2250, 2003.
12. **Faure JP, Petit I, Zhang K, Dutheil D, Doucet C, Favreau F, Eugene M, Goujon JM, Tillement JP, Mauco G, Vandewalle A, Hauet T.** Protective roles of polyethylene glycol and trimetazidine against cold ischemia and reperfusion injuries of pig kidney graft. *Am J Transplant* 4: 495–504, 2004.
13. **Goujon JM, Hauet T, Menet E, Levillain P, Babin P, Carretier M.** Histological evaluation of proximal tubule cell injury in isolated perfused pig kidneys exposed to cold ischemia. *J Surg Res* 82: 228–233, 1999.
14. **Hauet T, Goujon JM, Baumert H, Petit I, Carretier M, Eugene M, Vandewalle A.** Polyethylene glycol reduces the inflammatory injury due to cold ischemia/reperfusion in autotransplanted pig kidneys. *Kidney Int* 62: 654–667, 2002.
15. **Hauet T, Goujon JM, Vandewalle A, Baumert H, Lacoste L, Tillement JP, Eugene M, Carretier M.** Trimetazidine reduces renal dysfunction by limiting the cold ischemia/reperfusion injury in autotransplanted pig kidneys. *J Am Soc Nephrol* 11: 138–148, 2000.
16. **Hauet T, Baumert H, Amor IB, Gibelin H, Tallineau C, Eugene M, Tillement JP, Carretier M.** Pharmacological limitation of damage to renal medulla after cold storage and transplantation by trimetazidine. *J Pharmacol Exp Ther* 292: 254–260, 2000.
17. **Heinzelmann M, Mercer-Jones MA, Passmore JC.** Neutrophils and renal failure. *Am J Kidney Dis* 34: 384–399, 1999.
18. **Jassem W, Fuggle SV, Rela M, Koo DD, Heaton ND.** The role of mitochondria in ischemia/reperfusion injury. *Transplantation* 73: 493–499, 2002.
19. **Junqueira L, Bignoles G, Brentani R.** Picro Sirius staining plus polarization microscopic, a specific method for collagen detection in tissue sections. *Histochem J* 11: 447–455, 1979.
20. **Kantor P, Lucien A, Kozak R, Lopaschuk G.** The antianginal drug trimetazidine shifts cardiac energy metabolism from fatty acid oxidation to glucose oxidation by inhibiting mitochondrial long-chain 3-ketoacyl coenzyme A thiolase. *Circ Res* 86: 580–588, 2000.
21. **Koppel J, Loyer P, Maucuer A, Rehak P, Manceau V, Guguen-Guillouzo C, Sobel A.** Induction of stathmin expression during liver regeneration. *FEBS Lett* 331: 65–70, 1993.
22. **Li C, Jackson RM.** Reactive species mechanisms of cellular hypoxia-reoxygenation injury. *Am J Physiol Cell Physiol* 282: C227–C241, 2002.
23. **Marzilli M.** Cardioprotective effects of trimetazidine: a review. *Curr Med Res Opin* 19: 661–672, 2003.
24. **Maupoil V, Rochette L, Tabard A, Clauser P, Harpey C.** Direct measurement of free radical generation in isolated rat heart by electron paramagnetic resonance spectroscopy: effect of trimetazidine. *Adv Exp Med Biol* 264: 373–376, 1990.
25. **Morillas Blasco PJ, Hernándiz Martinez A, Azorín Villena I, Portolés Sanz M, Pallarés Carratalá V, Bertomeu Martínez V, Capdevila Carbonell C, Aguilar Llopis A, Cosín Aguilar J.** Mitochondrial changes induced by trimetazidine in the myocardium. *Med Sci Monit* 11: 162–167, 2005.

26. **Newaz MA, Oyekan AO.** Vascular response to endothelin-1, angiotensin-II and U46619 in glycerol-induced acute renal failure. *J Cardiovasc Pharmacol* 38: 569–577, 2001.

27. **Ortiz A, Justo P, Sanz A, Lorz C, Egido J.** Targeting apoptosis in acute tubular injury. *Biochem Pharmacol* 66: 1589–1594, 2003.

28. **Ozden A, Aybek Z, Saydam N, Calli N, Saydam O, Duscan E, Guner G.** Cytoprotective effect of trimetazidine on 75 min warm ischemia-reperfusion injury in rats. *Eur Surg Res* 30: 227–234, 1998.

29. **Penfield JG, Wang Y, Li S, Kielar MA, Sicher SC, Jeyarajah DR, Lu CY.** Transplant surgery injury recruits recipient MHC class II-positive leukocytes into the kidney. *Kidney Int* 56: 1759–1769, 1999.

30. **Rowlands DC, Williams A, Jones NA, Guest SS, Reynolds GM, Barber PC, Brown G.** Stathmin expression in a feature of proliferating cells of most, if not all, cell lineages. *Lab Invest* 72: 100–113, 1995.

31. **Rubin CI, Atweh GF.** The role of stathmin in the regulation of the cell cycle. *J Cell Biol* 93: 242–250, 2004.

32. **Ruiz-Meana M, Garcia-Dorado D, Julia M, Gonzalez MA, Inserte J, Soler-Soler J.** Pre-treatment with trimetazidine increases sarcolemmal mechanical resistance in reoxygenated myocytes. *Cardiovasc Res* 32: 587–592, 1996.

33. **Sentex E, Sergiel JP, Lucien A, Grynberg A.** Trimetazidine increases phospholipid turnover in ventricular myocyte. *Mol Cell Biochem* 175: 153–162, 1997.

34. **Siegel NJ, Shah SV.** Acute renal failure: directions for the next decade. *J Am Soc Nephrol* 14: 2176–2177, 2003.

35. **Tselepis A, Doulias P, Lourida E, Glantzounis G, Tsimoyiannis E, Galaris D.** Trimetazidine protects low-density lipoproteins from oxidation and cultured cells exposed to H_2O_2. *Free Radic Biol Med* 30: 1357–1364, 2001.

36. **Vetterlein F, Petho M, Schmidt G.** Distribution of capillary blood flow in rat kidney during postischemic renal failure. *Am J Physiol* 20: 510–519, 1986.

37. **Villanueva S, Cespedes, Vio CP.** Ischemic acute renal failure induces the expression of a wide range of nephrogenic proteins. *Am J Physiol Regul Integr Comp Physiol* 290: R861–R870, 2006.

38. **Williams FM, Tanda K, Kus M, Wiliams TJ.** Trimetazidine inhibits neutrophil accumulation after myocardial ischemia and reperfusion in rabbits. *J Cardiovasc Pharmacol* 22: 828–833, 1993.

39. **Witzgall R, Brown D, Schwarz C, Bonventre JV.** Localization of proliferating cell nuclear antigen, vimentin, c-Fos, and clusterin in the postischemic kidney. Evidence for a heterogenous genetic response among nephron segments, and a large pool of mitotically active and dedifferentiated cells. *J Clin Invest* 93: 2175–2188, 1994.

40. **Yin RX, Liang WW, Liu TW, Tao XZ, Zhu LG, Al-Ghazali R.** Inhibitory effect of trimetazidine on cardiac myocyte apoptosis in rabbit model of ischemia-reperfusion (Abstract). *Chin Med Sci* 19: 242, 2004.

41. **Ysebaert DK, De Greef KE, Vercauteren SR, Ghielli M, Verpooten GA, Eyskens EJ, De Broe ME.** Identification and kinetics of leukocytes after severe ischaemia/reperfusion renal injury. *Nephrol Dial Transplant* 15: 1562–1574, 2000.

42. **Ysebaert DK, De Greef KE, De Beuf A, Van Rompay AR, Vercauteren S, Persy VP, De Broe ME.** T cells as mediators in renal ischemia/reperfusion injury. *Kidney Int* 66: 491–496, 2004.

43. **Yukselen V, Karaoglu AO, Yenisey C, Tuncyurek M, Ozutemiz O.** Trimetazidine reduces the degree of fibrosis in alkali burns of the esophagus. *J Pediatr Surg* 40: 505–509, 2005.

44. **Zahedi K, Wang Z, Barone S, Tehrani K, Yokota N, Petrovic S, Rabb H, Soleimani M.** Identification of stathmin as a novel marker of cell proliferation in the recovery phase of acute ischemic renal failure. *Am J Physiol Cell Physiol* 286: C1203–C1211, 2004.

45. **Zahedi K, Revelo MP, Barone S, Wang Z, Tehrani K, Citron DP, Bissler JJ, Rabb H, Soleimani M.** Stathmin-deficient mice develop fibrosis and show delayed recovery from ischemic-reperfusion injury. *Am J Physiol Renal Physiol* 290: F1559–F1567, 2006.